Impact of soil puddling intensity on the root system architecture of rice (*Oryza sativa* L.) seedlings

Huan Fang[a,b], Hui Rong[a,b], Paul D. Hallett[c], Sacha J. Mooney[d], Weijian Zhang[e], Hu Zhou[a,c,d*], Xinhua Peng[a*]

[a] *State Key Laboratory of Soil and Sustainable Agriculture, Institute of Soil Science, Chinese Academy of Sciences. No.71 East Beijing Road, Nanjing 210008, China*

[b] *University of Chinese Academy of Sciences, No.19A Yuquan Road, Beijing 100049, China*

[c] *School of Biological Sciences, University of Aberdeen, Aberdeen AB24 3UU, United Kingdom*

[d] *Division of Agricultural and Environmental Sciences, School of Biosciences, University of Nottingham, Sutton Bonington Campus, Loughborough, Leicestershire LE12 5RD, United Kingdom*

[e] *Institute of Crop Sciences, Chinese Academy of Agricultural Sciences, Beijing 100081, China*

[*] *Corresponding author*

Hu Zhou
Phone: 86(25) 86881221
Fax: 86(25) 86881000
E-mail: zhouhu@issas.ac.cn
and
Xinhua Peng
Phone: 86(25) 86881198
Fax: 86(25) 86881000
E-mail: xhpeng@issas.ac.cn

Abstract

Puddling of rice paddies is undertaken to create a soft soil bed for easy transplanting of rice seedlings, to control weeds and reduce water and nutrient leaching. There is a drive for less intense puddling because of its physical disturbance of soil, energy inputs and labour requirements, which may produce different soil physical conditions for root growth. The objective of this study was to investigate the influence of puddling intensity on soil structure and the subsequent impact on the growth of rice seedling roots. Three treatments with different puddling intensities were established: (1) No puddling; (2) Low and (3) High intensity puddling. The rice genotype, Nipponbare was grown in soil columns for 18 days. Soil bulk density, aggregate size distribution and three-dimensional (3D) macropore structure were measured. Two-dimensional root traits were determined by WinRhizo and 3D root traits were determined by X-ray Computed Tomography (CT). Our results show the percentage of large macroaggregates (> 2 mm) decreased by 69.6% ($P < 0.05$) for low intensity puddling and by 95.7% ($P < 0.05$) for high intensity puddling compared with that of no puddling. The macroporosity (> 0.03 mm) of no puddling was 2.3 times greater than low intensity puddling and 3.5 times greater than high intensity puddling. The total root lengths of no and low intensity puddling were 1.56-1.86 times greater than that of high intensity puddling. Large roots, including radicle and crown roots, were the same length regardless of puddling intensity. Our study demonstrates that intensive puddling can degrade soil structure, which consequently limits rice root growth.

Keywords: Puddling; Pore structure; Root architecture; Soil structure; X-ray

computed tomography

1. Introduction

Puddling is the most common tillage practice for lowland rice (*Oryza sativa* L.) cultivation in Asian countries (Bouman et al., 2007; Eickhorst and Tippkötter, 2009). Puddling breaks down and disperses soil aggregates into micro-aggregates and individual particles (Zhang et al., 2016), which helps with the creation of a soft soil bed for easy transplanting of rice seedlings, weed control and the reduction of water and nutrients leaching (Bouman et al., 2007; Kirchhof et al., 2011; Sharma and De Datta, 1985). Societal change in China has resulted in a rapid decrease in puddling intensity (Wang et al., 2017) as more large-scale family farms have emerged from the land-use right transfer from small-scale farms (Liu, 2018). Unlike the small-scale farmers who keep puddling the paddy fields for rice seedlings, larger scale operations often reduce puddling intensity to save on labour and energy costs, and to prepare fields rapidly to maximise the length of growing seasons. Some farmers have gone as far as implementing reduced and zero tillage in rice cultivation to achieve this (Wang et al., 2017). However, there is a lack of knowledge concerning how these drastic changes in preparing soil for rice paddy production affect the interactions between rice and soils. Yields can be maintained or sometimes improved with less intense puddling (Mohanty et al., 2004), which counters the common perception of many farmers (Wang et al., 2017).

Puddling has a significant effect on soil structure that may influence root growth. Previous studies have shown that the intensity of puddling influences the physical properties of paddy soil such as aggregate stability, bulk density, pore size distribution, penetration resistance, water retention and hydraulic conductivity (Mohanty et al., 2004; Mousavi et al., 2009; Rezaei et al., 2012; Yoshida and Adachi, 2002). These changes to soil physical properties due to puddling intensity likely affect rice root growth (Bengough et al., 2011; Kirchhof et al., 2000; Valentine et al., 2012; White and Kirkegaard, 2010) and yields, often contrary to what farmers may expect (Mohanty et al., 2004). Sharma and De Datta (1985) reported that intense puddling impeded root development and therefore led to a decline in yield. Other researchers have demonstrated that puddling can increase weeding efficiency and provide a better environment for nutrient uptake, leading to increased grain yield (Arora et al., 2006; Mohanty and Painuli, 2003; Mohanty et al., 2004; Singh et al., 2013; Subramanyam et al., 2007).

Both soil pore size distribution and aggregation are greatly affected by puddling, which can have a direct impact on crop yield due to the physical impacts on root growth and resource capture (Cairns et al., 2004). Much work in this area has focused on soil aggregates or bulk parameters such as bulk density and hydraulic conductivity (Rezaei et al., 2012), but a detailed analysis concerning the impact on the soil pore system has been largely ignored. The soil pore network has a profound influence on root growth, providing a continuous network of appropriately sized soil pores that provide growth channels for roots (Tracy et al., 2012b). In a previous study, we found that different pore structures had a large influence on root elongation and morphology, even if soil bulk densities were identical (Fang et al., 2018). This study explored impacts of hydraulic stress history, with X-ray Computed Tomography (CT) imaging using to quantify the 3D pore structure. Scope exists to further this noninvasive approach to explore puddling intensity impacts, coupled with visualization of the 3D root system, as applied to a wide range of crop species (Helliwell et al., 2013).

X-ray CT imaging provides micron resolution, 3D images of the interaction between soil structure and root system architecture. Compared to the destructive methods like root washing, CT imaging can examine undisturbed 3D root architecture, including branching characteristics and extension rate, which are inherently linked to conditions within the soil matrix (Tracy et al., 2010). At the same time, it provides information on soil pore structure and its capacity to serve as growth pathways for roots (Helliwell et al., 2017). The application of X-ray CT also has a number of disadvantages including the trade-off between spatial resolution and sample size (Zappala et al., 2013), which can limit the portion of the root system that is observable or the size of plants. Scans of 100-150 mm diameter samples are typically limited to about 50-80 μm resolution, so only the larger roots (e.g., radicle and crown roots) of cereal plants are clearly visible. With root washing, on the other hand, information concerning the radicle, crown roots and lateral roots can be collected, but the spatial arrangement of the roots is disturbed. Therefore, combining X-ray CT and root washing methods offers a better understanding of root system architecture (Tracy et al., 2012a).

The aim of this study was to explore the effect of different puddling intensities on soil physical properties and their influence on rice root development. Soil physical conditions were characterized by aggregate size distribution, bulk density and a detailed analysis of 3D pore structure by X-ray CT. Root system architecture was studied using X-ray CT imaging and root washing methods. Our hypothesis was that the destruction of soil aggregates and pore structure by puddling will decrease root length and branching. We also anticipated that a greater intensity of puddling will increase mechanical impedance. Our hypothesis is counter-intuitive to the common belief that greater puddling intensity produces better rice root growth. With new data, including easily accessible 3D visual images of root interactions with soil structure, a primary aim of this study is to demonstrate the benefits of less intense puddling in rice production. It addresses current changes in farming practices in China, as well as concerns about the impact of intense puddling on soil sustainability.

2. Materials and methods

2.1. Experimental design

Paddy soil (4.7% sand，67.2% silt and 28.1% clay) was obtained from the Institute of Red Soil, Jinxian County, Jiangxi Province, China (28°37′ N, 116°26′ E). The pH of the soil was 5.3. The soil organic carbon content was 24.8 g kg^{-1}. The total nitrogen (N), phosphorus (P) and potassium (K) content of the soil were 2.60 g kg^{-1}, 1.28 g kg^{-1}, 12.36 g kg^{-1}, respectively. The soil was air-dried and passed through a 5 mm sieve to retain some its inherent structure, whilst allowing for packing into small soil columns compatible with X-Ray CT scanning.

Soil treatments with different puddling intensities were formed in polyvinyl chloride (PVC) columns (inner diameter 48 mm, height 80 mm). To retain soil during the puddling process, two columns were taped together so that soil would not splash outside of the sample. Each stacked column had 200 g of soil loosely packed inside, with soil surface below the middle of the upper column to avoid soil falling out during stirring. The repacked soils were then saturated by placing the columns in a container and submerging in water for 72 h. They were then mixed with an electric mixer equipped with a 1000 W motor and two mixing blades. The rotating speed was 200 rpm. Different puddling intensities were simulated by changing stirring time, which was similar to puddling multiple times in the field. Three treatments with different puddling intensities were established: (1) no puddling; (2) low intensity puddling, 200 rpm for 2 min; and (3) high intensity puddling, 200 rpm for 8 min. After stirring, soils were equilibrated to -0.5 kPa in a sand table to allow the puddled soil to settle and consolidate. Once equilibrated, the upper columns and the soil within them were removed carefully, with the bottom columns retained for the experiment. There were 9 columns produced for each treatment, split into 6 replicates used to grow rice and the other 3 replicates for the measurement of soil aggregate size distribution. The rice (*Oryza sativa*) genotype, Nipponbare, was used in this study. Rice seeds were germinated on moist filter paper at 30 °C for 48 hours before being planted at 3 mm below the soil surface. All the columns were placed in a large container and kept flooded during the growing period. Plants were grown in a controlled greenhouse with day/night temperatures of 28/26 °C, a humidity of 60% and an 11 h photoperiod. The rice plants were grown for 18 days as the soil sample size required for X-Ray CT scanning restricted a longer growth period without edge affects adversely influencing root morphology. Soil bulk density was determined after rice harvest by collecting all the soils in the column and oven-drying at 105 ℃.

2.2. Aggregate size distribution

The aggregate size distribution after simulated puddling was determined using a sieving method modified from Elliott (1986). Briefly, a series of sieves were used to obtain four aggregate size fractions: 1) > 2 mm (large macroaggregates); 2) 0.25-2 mm (small macroaggregates); 3) 0.053-0.25 mm (microaggregates); 4) < 0.053 mm (silt and clay fractions). The sieves were manually moved up and down by about 3 cm a total of 50 times during 2 min. The aggregates remaining on each sieve were oven-dried at 105 °C until they reached a constant weight. The mean weight diameter (MWD) of the aggregates was calculated as follows:

$$\mathrm{MWD} = \sum_{i=1}^{n+1} \frac{r_{i-1} + r_i}{2} \times m_i$$

where r_i is the aperture size of the i^{th} sieve (mm), m_i is the mass proportion of the aggregate fraction remaining on the i^{th} sieve, and n is the number of sieves.

2.3. X-ray CT scanning and image processing

Soil columns were scanned using a Phoenix Nanotom X-ray μ-CT (GE, Sensing and Inspection Technologies, GmbH, Wunstorf, Germany) at the Institute of Soil Science, Chinese Academy of Sciences. The voltage was 110 kV, the current was 110 μA, the exposure time was 1250 ms, and a 0.1 mm Cu filter was used to reduce the beam hardening effect. A total of 1200 projection images were collected during the rotation of each sample. To improve image quality, each projection image was collected three times, with the first projection image skipped and the average of the last two projections saved as one projection image. The voxel size was 0.03 mm. Slices were reconstructed with Datos|× 2.0 software using the filtered back-projection algorithm. The slices were saved as 16-bit tiff format.

X-ray CT image data analysis is extremely time consuming, so only three of the six replicates of each treatment were randomly selected and scanned at day 0 and day 18. Soil columns were placed on dry sands for 1 hour before scanning to drain the soil water in the macropores because a high proportion of water-filled pores can impact image quality, especially for root segmentation (Zappala et al., 2013). CT images from day 0 were used to analyze soil pore structure using imageJ (Version 1.50e). The image stack of each sample was cropped to a region of interest (ROI) of 700 × 700 pixels (21 × 21 mm) and a depth of 700 continuous slices (21 mm). Cropping the images and reducing the size of the stacks was necessary to avoid artefacts detected at the edges or top and bottom of columns such as those caused by use of a cone X-ray beam or beam hardening (Deurer et al. 2009; Mooney et al. 2006). Images were segmented using a 'Default' thresholding method, a variation on the 'IsoData' method where the average of the object and background image are used to compute the threshold. Porosity and pore size distribution were computed using the 'thickness' plugin in ImageJ. This approach fits the largest sphere inside the 3D pore space that touches the bordering soil matrix and then measures the sphere diameter, which is regarded as the corresponding "pore size". The global connectivity (Γ) of soil pore networks can be defined as follows:

$$\Gamma = \frac{\sum_{i=0}^{n}(V_i^2)}{(\sum_{i=0}^{n} V_i)^2}$$

The Γ measures the probability of pores belonging to the same pore. A Γ equal to 1 indicates that all pores are connected in one percolating pore, whereas a Γ close to 0 indicates that pores with similar size are scattered (Hovadik and Larue, 2007). V_i is the volume of the ith macropore.

CT images from day 18 were analysed to quantify root architecture. Root systems were segmented using the "Region Growing" tool in VG StudioMax 2.1 software. The root length, volume, surface area, mean diameter and tortuosity of root path (the ratio of actual path length divided by the shortest possible path) were measured on the extracted root system. The root volume and surface area were obtained from VG StudioMax 2.1. The root length and the tortuosity of root path were obtained using 'skeleton' plugin of ImageJ. The mean diameter was computed using the 'thickness' plugin in imageJ.

2.4. Root washing

After CT scanning, roots were carefully washed from the soil. Roots with soil were placed on a sieve (aperture size 0.5 mm) and carefully washed with tap water to remove soil particulate material. All the soil material in the column was collected and oven-dried at 105 °C to determine soil bulk density. Root samples from each core were placed in a plexiglas tray (100 by 100 mm) containing a 4 to 6 mm deep layer of water and spread out with plastic tweezers to minimize root overlapping. Roots were scanned using an Expression 10000XL scanner (Epson, Suwa, Japan) and grayscale images (800 DPI) of roots were obtained. Based on manual measurement, a threshold diameter of 0.2 mm was chosen to separate larger roots (including radical and crown roots) and lateral roots. Total root length, root surface area, root volume, average diameter, and tip numbers were determined using WinRhizo (Version 2013e) (Regent Instrument Canada Inc.).

2.5. Statistical analysis

Data were checked for normality with probability plots. One-way ANOVA and post hoc analysis were conducted by the Fisher's protected least significant difference (LSD) procedure with SPSS 24.0 to evaluate for significant differences between treatments ($P < 0.05$).

3. Results

3.1. Puddling intensity effect on aggregate size distribution and bulk density

The impact of puddling intensity on soil aggregate size distribution is shown in Table 1. Puddling had significant impacts on disrupting macroaggregates (> 0.25 mm) ($P < 0.05$) and producing microaggregates (< 0.25 mm) ($P < 0.05$). The percentage of aggregates > 2 mm with no puddling was 3.4 and 20.1 times greater than for low and high puddling intensity, respectively ($P < 0.05$). The percentage of < 0.053 mm aggregates following no puddling was 45.8% and 54.9% less than that of low and high puddling intensity, respectively ($P < 0.05$). The MWD for no puddling was 2.1 and 3.5 times greater than that of low and high puddling intensity, respectively ($P < 0.05$). Puddling increased bulk density by 10.6% for low intensity and 14.1% for high intensity compared to no puddling ($P < 0.05$) (Table 1).

3.2. Puddling intensity effect on macropores

Representative longitudinal cross-section images of the different treatments are shown in Fig. 1. Puddling clearly disrupted the pore structure, resulting in lower bulk porosities (Table 1) and more small pores (Fig. 1). Compared to no puddling, the number of large pores decreased with increasing puddling intensity. The connected inter-aggregate pores were destroyed by puddling, producing isolated vesicular pores after low intensity puddling. After high intensity puddling, most of the larger macropores had disappeared (Figs. 1 & 2). The circular pores following puddling were not connected at the image resolution in this study (Fig. 1). The trends observed in the 2D images were also shown in the representative 3D soil structure (Fig. 2).

Quantitative analyses of the 3D macropore system indicated puddling decreased soil macroporosity and macropore size, with the impacts being greater for high intensity than low intensity puddling (Fig. 3). The cumulative macroporosity with no puddling was 2.3 time greater than for low intensity puddling and 3.5 times greater than for high intensity puddling (Fig. 3b). Over a broad range of pores size intervals (0.03-2.4 mm) no puddling had much greater porosity than the two puddled treatments (Fig. 3a). These results confirmed our hypothesis that puddling destroys soil macropores. From the cumulative pore size distribution, low intensity and high intensity puddling started to deviate from each other at > 0.6 mm pores, reaching a difference of 3.9 times in total porosity between 0.6 mm and 2.4 mm pore sizes (Fig. 3b). The global connectivity (Γ) of macropores decreased with increased puddling intensity (Table 1). The pore connectivity of high intensity puddling was significantly less than that of no puddling ($P < 0.05$) (Table 1).

3.3. Puddling intensity effect on root traits

In 3D root images from X-ray CT imaging, information including the spatial position and 3D architecture of the roots was obtained (Fig. 4). Due to the limitation of image resolution, the CT imaging technique only revealed larger roots including radicle and crown roots, with smaller lateral roots not detectable. Quantitative analysis of CT images found no significant difference in the traits of detected roots, including root length, diameter, surface area, volume, and tortuosity among the treatments (Table 2).

Most roots could be detected following washing from the soil (Fig. 5) and analysis with WinRhizo, with very good agreement of the root length of roots > 0.2 mm between this approach and X-Ray CT imaging (Tables 2 & 3). Other root traits such as volume and surface area were much greater by root washing analysis. Larger roots (> 0.2 mm) quantified by root washing had similar traits regardless of puddling intensity ($P > 0.05$) (Table 3). Smaller lateral roots (< 0.2 mm) decreased with increasing puddling intensity (Table 3), with 1.55 times greater total root length for no puddling versus high intensity puddling. The surface area of small lateral roots for no puddling was 1.60 times greater than that of the high intensity puddling ($P < 0.05$). Small lateral roots had a similar number of tips and volume regardless of puddling intensity ($P > 0.05$) (Table 3).

For the entire root system, the total root length with no puddling was 1.43 times greater than that with high intensity puddling ($P < 0.05$). The average root diameters of the low and high intensity puddling were 12.2% and 16.8% greater than that of no puddling ($P < 0.05$) (Table 3), respectively.

4. Discussion

Puddling intensity has a large impact on soil physical structure that affects the root architecture of rice. Despite mechanically disrupting inherent macro-aggregates to micro-aggregates with an intention to 'loosen' the soil, pluviation of the soil and subsequent consolidation produces the counter-intuitive response with soil bulk density increasing alongside increasing puddling intensity (Table 1). Puddling destroyed macro-aggregates to micro-aggregates or even dispersed soil particles, resulting in decreased aggregate sizes (Table 1). This effect was more pronounced when the puddling intensity was increased by a longer puddling time (Table 1), as reported in previous studies (Kirchhof et al., 2000; Deng et al., 2014; Zhang et al., 2016).

Our study provided unprecedented visualization of the impact of puddling intensity on the resulting pore structure, facilitated through X-ray CT imaging. Puddling intensity not only decreased soil macroporosity (> 0.03 mm), producing smaller pores with less total macropore volume (Fig. 3), but also altered pore morphology (Figs. 1 & 2) and decreased pore connectivity (Table 1). This supports findings by Lal and Shukla (2004) and Chauhan et al. (2012) who also pointed out puddling caused the loss of both inter- and intra- aggregate macropores. Due to the difficulty of sampling soil after puddling (Sharma and De Datta, 1985), few studies have sought to directly investigate the soil pore structure after puddling. An advantage of X-ray CT imaging is the ability to investigate 3D pore morphology, including shape and connectivity besides porosity. The decreased macroporosity and connectivity in the puddled soil is likely to reduce gas exchange and water conductivity, and impact plant root growth (Sharma and De Datta, 1985).

The greater bulk density with increasing puddling intensity agrees with some earlier experiments (Kukal and Aggarwal, 2003; Lima et al., 2009), but some other studies have found the converse in that puddling decreased soil bulk density (Rezaei et al., 2012; Zhang et al., 2016). This discrepancy mainly results from the time of sampling. Kukal and Aggarwal (2003) and Lime et al. (2009) sampled after harvest, whereas in the other two studies (Rezaei et al., 2012; Zhang et al., 2016) soil bulk density was measured shortly after puddling. Zhang et al. (2013) found that soil bulk density increased with wetting and drying cycles over the course of a rice season. One objective of puddling is to create a soft soil bed for easy rice transplanting (Bouma et al., 2007; Kirchhof et al., 2011) so that the paddy soil bulk density is quite low and soil strength is weak after puddling. However, the dispersing of soil aggregates and particles is at a cost of losing macropores (Figs. 1 & 2) after puddling, resulting in a higher bulk density developing following wetting and drying cycles (Table 1). Adopting less intensive puddling, as is increasingly common with societal changes in China, may lead to more favourable soil physical conditions for root growth.

We found only minimal impact of puddling intensity on large root (radical and crown roots) architecture for the 18 day old rice plants studied (Table 2). However, the increased root length and decreased root diameter observed with decreasing puddling intensity follows a favourable trajectory. Root system architecture is strongly dependent on genotype, but soil conditions can have an even greater impact (Bengough et al., 2011). Soil structure determines the balance of axial and radial pressures on the individual root tip, and hence the root elongation response (Bengough, 2012). Lipiec et al. (2012) demonstrated root elongation and anatomy to be quite plastic in response to the local soil environment around the roots. During elongation, the root tip is pushed forward into the soil and has to overcome the mechanical resistance of the soil (Hodge et al., 2009). Kolb et al. (2017) reported that roots respond differently to different size class of soil aggregates/particles depending on whether the root can deform or dislodge the aggregates/particles. If not, roots may change their trajectory to exploit looser soil areas nearby or grow through macropores (Colombi et al., 2017). Roots that are able to penetrate the soil reorganize particles, which in turn modifies the distribution of pores and the local soil packing fraction which affects further root growth (Whiteley and Dexter, 1984). Despite large differences in soil structure caused by puddling intensity in our study, root system architecture of > 0.2 mm roots was not affected (Tables 2 & 3), likely due to the low penetration resistance of the flooded soil (Kukal and Aggarwal, 2003). Lateral roots (< 0.2 mm), however, were suppressed with increasing puddling intensity (Table 3). For no puddling, they were longer and more tortuous than those of the puddled soils (Fig. 5, Table 3). Two processes could drive these differences. The lateral roots may be suppressed under poor aeration conditions (Ben-Noach and Friedman, 2018). The intensive puddling caused smaller and more disconnected macropores (Figs. 1 & 2), which strongly limits soil air diffusion. On the other hand, macropores can also serve as growth pathways for roots, so their destruction through puddling could create another restriction. Colombi et al. (2017) showed roots of wheat, soybean and maize grew preferentially towards artificially created vertical macropores (1.25 mm) in the soil. Recently, our previous study (Fang et al., 2018) observed that macropores (> 0.03 mm) greatly promoted rice root elongation and branching. These studies indicated that macropores provided a favorable environment for root growth with respect to better soil aeration and reduced penetration resistance. So far, the influence of the size of macropores remains unclear. Further detailed investigations of macropore-root interaction are still needed, which will be facilitated greatly by rapidly growing technologies like X-ray CT. In our system, the 3D root system architecture from X-ray CT images was limited to large roots due to resolution, but by using smaller size samples or higher resolution obtainable with Synchrotron CT, much smaller roots can be visualized (Koebernick et al., 2017), though this is at the expense of considering a larger part of the total root system architecture.

This study was limited to rice seedlings grown in a repacked soil that was carefully manipulated under controlled conditions. At field conditions, the structure of paddy soil is very dynamic during the growing season due to wetting/drying cycles (Mohanty et al., 2004). Two questions need to be further studied: (1) the response of the puddled soil to wetting/drying cycles; and (2) their effect on rice roots considered over the whole growing season, and also on the resulting rice yield. Only when these questions are clearly answered can useful techniques be offered to farmers to better manage their paddy fields. However, this initial study suggests decreasing puddling intensity may not only save on labour and energy, but also produce favorable conditions for rice root growth.

5. Conclusions

Puddling can destroy macroaggregates and macropores, leading to an increased bulk density, and decreased soil MWD, macroporosity and pore connectivity. These effects are enhanced as puddling intensity increases. Puddling did not significantly influence the growth of radicle or crown roots, but high intensity puddling significantly reduced the length and surface area of lateral roots in the young plants studied here. Further research is needed to explore more mature plants and take account of the dynamic nature of soil structure over the course of a growing season. Moreover, the interaction between soil structure and root system architecture of rice genotypes with contrasting root traits may help identify varieties more suited to China's shift towards less intensive paddy soil puddling.

Acknowledgments

This work was financially supported by the National Natural Science Foundation of China (41471183, 41877022, 41725004, 41571130053), the National Key Research and Development Program (2016YFD0300906), the Chinese National Basic Research Program (2015CB150400) and the UK Natural Environmental Research Council (NERC: Code: NE/N007611/1).

References

Arora, V.K., Gajri, P.R., Uppal, H.S., 2006. Puddling, irrigation, and transplanting-time effects on productivity of rice–wheat system on a sandy loam soil of Punjab, India. Soil Tillage Res. 85, 212-220.

Bengough, A.G., 2012. Root elongation is restricted by axial but not by radial pressures: so what happens in field soil?. Plant Soil 360, 15-18.

Bengough, A.G., McKenzie, B.M., Hallett, P.D., Valentine, T.A., 2011. Root elongation, water stress, and mechanical impedance: a review of limiting stresses and beneficial root tip traits. J. Exp. Bot. 62, 59-68.

Ben-Noach, I., Friedman, S.P., 2018. Review and evaluation of root respiration and of natural and agricultural processes of soil aeration. Vadose Zone J. 17, 170119.

Bouman, B.A.M., Lampayan, R.M., Tuong, T.P., 2007. Water Management in Irrigated Rice: Coping with Water Scarcity. International Rice Research Institute, Los Baños, Philippines.

Cairns, J.E., Audebert, A., Townend, J., Price, A.H., Mullins, C.E., 2004. Effect of soil mechanical impedance on root growth of two rice varieties under field drought stress. Plant Soil 267, 309–318.

Chauhan, B.S., Mahajan, G., Sardana, V., Timsina, J., Jat, M.L., 2012. Productivity and Sustainability of the Rice–Wheat Cropping System in the Indo-Gangetic Plains of the Indian subcontinent: Problems, Opportunities, and Strategies. Academic Press, pp 315-369.

Colombi, T., Braun, S., Keller, T., Walter, A., 2017. Artificial macropores attract crop roots and enhance plant productivity on compacted soils. Sci. Total Environ. 574, 1283-1293.

Deng, C., Teng, X.L., Peng, X.H., Zhang, B., 2014. Effects of simulated puddling intensity and pre-drying on shrinkage capacity of a paddy soil under long-term fertilization. Soil Tillage Res. 140, 135-143.

Deurer, M., Grinev, D., Young, I., Clothier, B.E., Müller, K., 2009. The impact of soil carbon management on soil macropore structure: a comparison of two apple orchard systems in New Zealand. Eur J. Soil Sci. 60:945-955

Eickhorst, T., Tippkötter, R., 2009. Management-induced structural dynamics in paddy soils of south east China simulated in microcosms. Soil Tillage Res. 102. 168-178.

Elliott, E.T., 1986. Aggregate Structure and Carbon, Nitrogen, and Phosphorus in Native and Cultivated Soils 1. Soil Sci. Soc. Am. J. 50, 627-633.

Fang, H., Zhou, H., Norton, G.J., Price, A.H., Raffan, A.C., Mooney, S.J., Peng, X.H., Hallett, P.D., 2018. Interaction between contrasting rice genotypes and soil physical conditions induced by hydraulic stresses typical of alternate wetting and drying irrigation of soil. Plant Soil 430, 233-243.

Helliwell, J.R., Sturrock, C.J., Grayling, K.M., Tracy, S.R., Flavel, R.J., Young, I.M., Whalley, W.R., Mooney, S.J., 2013. Applications of X-ray computed tomography for examining biophysical interactions and structural development in soil systems: a review. Eur. J. Soil Sci. 64, 279-297.

Helliwell, J.R., Sturrock, C.J., Mairhofer, S., Craigon, J., Ashton, R.W., Miller, A.J., Whalley, W.R., Mooney, S.J., 2017. The emergent rhizosphere: imaging the development of the porous architecture at the root-soil interface. Sci. Rep. 7,14875.

Hodge, A., Berta, G., Doussan, C., Merchan, F., Crespi, M., 2009. Plant root growth, architecture and function. Plant Soil 321, 153-187.

Hovadik, J. M., & Larue, D. K., 2007. Static characterizations of reservoirs: refining the concepts of connectivity and continuity. Petrol. Geosci. 13, 195-211.

Kirchhof, G., Priyono, S., Utomo, W.H., Adisarwanto, T., Dacanay, E.V., So, H.B., 2000. The effect of soil puddling on the soil physical properties and the growth of rice and post-rice crops. Soil Tillage Res. 56, 37-50.

Kirchhof, G., Tuong, T.P., So, H.B., 2011. Puddling: effect on soil physical properties and crops. Springer, pp 667-668.

Koebernick, N., Daly, K.R., Keyes, S.D., George, T.S., Brown, L.K., Raffan, A., Cooper, L.J., Naveed, M., Bengough, A.G., Sinclair, I., Hallett, P.D., Roose, T., 2017. High-resolution synchrotron imaging shows that root hairs influence rhizosphere soil structure formation. New Phytol. 216, 124-135.

Kolb, E., Legué, V., Bogeat-Triboulot, M.B., 2017. Physical root–soil interactions. Phys. Biol. 14, 065004.

Kukal, S.S., Aggarwal, G.C., 2003. Puddling depth and intensity effects in rice–wheat system on a sandy loam soil: I. Development of subsurface compaction. Soil Tillage Res. 72, 1-8.

Lal, R., Shukla, M.K., 2004. Principles of soil physics. CRC Press.

Lima, A.C.R., Hoogmoed, W.B., Pauletto, E.A., Pinto, L.F.S., 2009. Management systems in irrigated rice affect physical and chemical soil properties. Soil Tillage Res. 103, 92-97.

Lipiec, J., Horn, R., Pietrusiewicz, J., Siczek, A., 2012. Effects of soil compaction on root elongation and anatomy of different cereal plant species. Soil Tillage Res.

121, 74-81.

Liu, M., 2018. A review of Chinese rural land circulation. Rural Econ. Sci-Technol. 29, 23-28 (In Chinese).

Mohanty, M., Painuli, D.K., 2003. Land preparatory tillage effect on soil physical environment and growth and yield of rice in a Vertisol. J. Indian Soc. Soil Sci. 51, 223-228.

Mohanty, M., Painuli, D.K., Mandal, K.G., 2004. Effect of puddling intensity on temporal variation in soil physical conditions and yield of rice (Oryza sativa L.) in a Vertisol of central India. Soil Tillage Res. 76, 83-94.

Mooney, S.J., Morris, C., Berry, P.M., 2006. Visualization and quantification of the effects of cereal root lodging on three-dimensional soil macrostructure using X-ray computed tomography. Soil Sci. 171, 706-718.

Mousavi, S.F., Yousefi-Moghadam, S., Mostafazadeh-Fard, B., Hemmat, A., Yazdani, M.R., 2009. Effect of puddling intensity on physical properties of a silty clay soil under laboratory and field conditions. Paddy Water Environ. 7, 45-54.

Rezaei, M., Tabatabaekoloor, R., Mousavi Seyedi, S.R., Aghili Nategh, N., 2012. Effects of puddling intensity on the in-situ engineering properties of paddy field soil. Aust. J. Agr. Eng. 3, 22-26.

Sharma, P.K., De Datta, S.K., 1985. Effects of puddling on soil physical properties and processes. Soil physics and rice. IRRI, Los Baños, Philippines, pp 217-234.

Singh, V.K., Dwivedi, B.S., Shukla, A.K., Meena, M.C., 2013. Effect of pre-puddling tillage and puddling intensities on soil physico-chemical properties and rice-wheat system productivity on a Typic Ustochrept of Indo-Gangetic Plains. J. Soil Water Conserv. 12, 291-300.

Subramanyam, D., Reddy, C.R., Reddy, D.S., 2007. Influence of puddling intensity and water-management practices on weed dynamics and yield of transplanted rice (*Oryza sativa*). Indian J. Agron. 52, 225-230.

Tracy, S.R., Black, C.R., Roberts, J.A., McNeill, A., Davidson, R., Tester, M., Samec, M., Korošak, D., Sturrock, C., Mooney, S.J., 2012a. Quantifying the effect of soil compaction on three varieties of wheat (Triticum aestivum L.) using X-ray micro computed tomography (CT). Plant Soil 353, 195-208.

Tracy, S.R., Black, C.R., Roberts, J.A., Sturrock, C., Mairhofer, S., Craigon, J., Mooney, S.J., 2012b. Quantifying the impact of soil compaction on root system architecture in tomato (Solanum lycopersicum) by X-ray micro-computed tomography. Ann. Bot. 110, 511-519.

Tracy, S.R., Roberts, J.A., Black, C.R., McNeill, A., Davidson, R., Mooney, S.J., 2010.

The X-factor: visualizing undisturbed root architecture in soils using X-ray computed tomography. J. Exp. Bot. 61, 311-313.

Valentine, T.A., Hallett, P.D., Binnie, K., Young, M.W., Squire, G.R., Hawes, C., Bengough, A.G., 2012. Soil strength and macropore volume limit root elongation rates in many UK agricultural soils. Ann. Bot. 110, 259-270.

Wang, W., Peng, S., Liu, H., Tao, Y., Huang, J., Cui, K., Nie, L., 2017. The possibility of replacing puddled transplanted flooded rice with dry seeded rice in central China: A review. Field Crops Res. 214, 310-320.

White, R.G., Kirkegaard, J.A., 2010. The distribution and abundance of wheat roots in a dense, structured subsoil–implications for water uptake. Plant Cell Environ. 33, 133-148.

Whiteley, G.M., Dexter, A.R., 1984. Displacement of soil aggregates by elongating roots and emerging shoots of crop plants. Plant Soil 77, 131-140.

Yoshida, S., Adachi, K., 2002. Influence of puddling intensity on the water retention characteristic of clayey paddy soil. 17th WCSS, 14–21 August 2002, Thailand, Symposium No. 53, Paper No. 235, pp 1-8.

Zappala, S., Mairhofer, S., Tracy, S.R., Sturrock, C.J., Bennett, M., Pridmore, T., Mooney, S.J., 2013. Quantifying the effect of soil moisture content on segmenting root system architecture in X-ray computed tomography images. Plant Soil 370, 35-45.

Zhang, Z.B., Peng, X.H., Wang, L.L., Zhao, Q.G., Lin, H., 2013. Temporal changes in shrinkage behavior of two paddy soils under alternative flooding and drying cycles and its consequence on percolation. Geoderma 192, 12-20.

Zhang, Z.B., Zhou, H., Lin, H., Peng, X.H., 2016. Puddling intensity, sesquioxides, and soil organic carbon impacts on crack patterns of two paddy soils. Geoderma 262, 155-164.

Table 1. Effects of puddling on the soil aggregate size distribution, mean weight diameter (MWD), and soil bulk density. Numbers in brackets are standard error of the mean. Different lowercases indicate that the means of different treatments are significantly different (*P* < 0.05).

Puddling Intensity	Aggregate size distribution (g g^{-1})				MWD (mm)	Bulk density (g cm^{-3})	Γ
	>2 mm	0.25-2 mm	0.05-0.25 mm	<0.05 mm			
No Puddling	0.23(0.02)a	0.38(0.01)a	0.17(0.01)b	0.22(0.02)c	1.17(0.06)a	0.96(0.01)c	0.017(0.006)a
Low	0.07(0.01)b	0.35(0.02)a	0.18(0.01)ab	0.40(0.02)b	0.57(0.01)b	1.06(0.01)b	0.008(0.002)ab
High	0.01(0.01)c	0.31(0.01)b	0.20(0.01)a	0.48(0.01)a	0.33(0.01)c	1.10(0.01)a	0.004(0.001)b

Table 2. Effects of puddling on the architecture of radicle and crown roots quantified with X-ray CT imaging. Numbers in brackets are standard error of the mean. Different lowercases indicate that the means of different treatments are significantly different ($P < 0.05$).

Puddling Intensity	Root length (cm)	Root diameter (mm)	Root surface area (cm^2)	Root volume (cm^3)	Root tortuosity
No Puddling	120(8)a	0.35(0.03)a	12.3(0.8)a	0.12(0.01)a	1.22(0.01)a
Low	130(12)a	0.39(0.01)a	13.1(0.8)a	0.12(0.01)a	1.23(0.01)a
High	129(20)a	0.37(0.03)a	11.8(2.4)a	0.11(0.03)a	1.23(0.01)a

Table 3. Effects of puddling on the architecture of roots. Numbers in brackets are standard error of the mean. Different lowercases indicate that the means of different treatments are significantly different ($P < 0.05$).

	Puddling Intensity	Root length (cm)	Root diameter (mm)	Root surface area (cm^2)	Root volume (cm^3)	Number of tips
All roots	No Puddling	494(54)a	0.19(0.01)b	26.1(2.6)a	0.30(0.01)a	1807(107)a
	Low	416(13)ab	0.21(0.01)a	24.6(0.9)a	0.30(0.02)a	1628(129)a
	High	345(54)b	0.22(0.01)a	21.0(2.5)a	0.27(0.03)a	1464(112)a
Radicle and crown roots (diameter > 0.2 mm)	No Puddling	121(10)a	NA	17.7(1.5)a	0.29(0.01)a	31(4)a
	Low	121(5)a	NA	17.7(0.8)a	0.28(0.02)a	38(5)a
	High	104(11)a	NA	15.8(1.5)a	0.26(0.03)a	35(5)a
Lateral roots (diameter < 0.2 mm)	No Puddling	373(46)a	NA	8.4(1.2)a	0.02(0.003)a	1776(106)a
	Low	295(10)ab	NA	7.0(0.5)ab	0.02(0.002)a	1590(127)a
	High	241(43)b	NA	5.2(1.0)b	0.01(0.003)a	1429(115)a

Figure captions

Figure 1. Vertical images of soil cores from different puddling intensities. Dark color indicates pore space, light gray indicates soil matrix.

Figure 2. Three-dimensional images of soil cores from different puddling intensities. Light color indicates pores, dark color indicates soil matrix. Sample size length is 21 mm.

Figure 3. Effects of puddling intensity on the soil pore size distribution (a) and cumulative pore size distribution (b) quantified using X-ray CT imaging. The shaded areas are the standard error of the mean.

Figure 4. Representative three-dimensional root architecture acquired with X-ray CT imaging from different puddling intensities.

Figure 5. Representative two-dimensional root images from different puddling intensities.

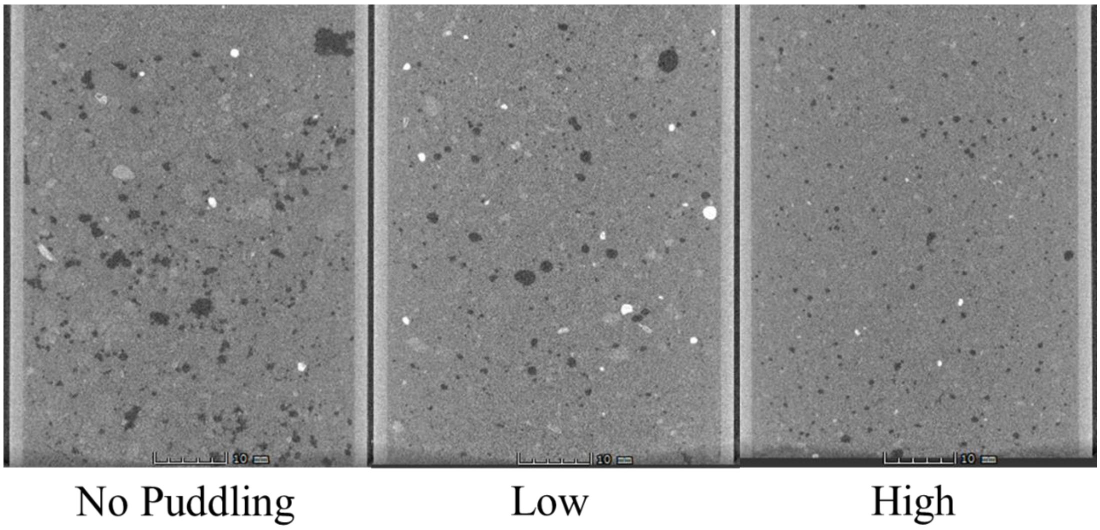

Figure 1. Vertical images of soil cores from different puddling intensities. Dark color indicates pore space, light gray indicates soil matrix.

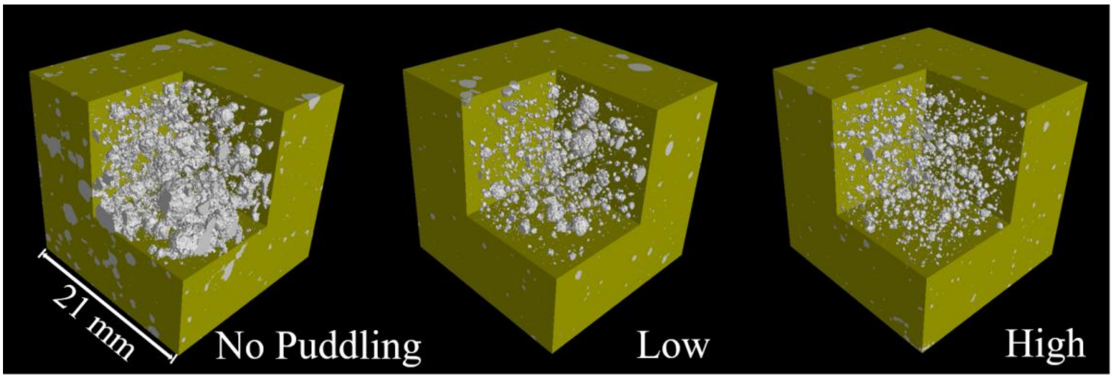

Figure 2. Three-dimensional images of soil cores from different puddling intensities. White color indicates pores, olive green color indicates soil matrix. Sample size length is 21 mm.

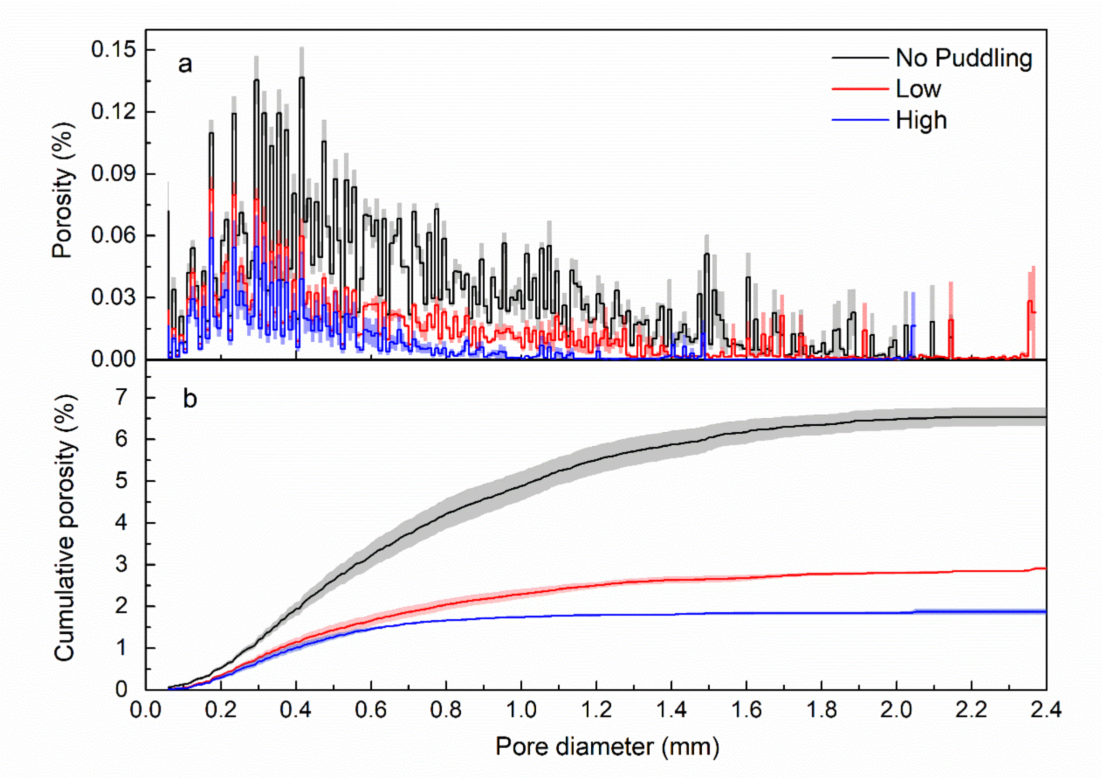

Figure 3. Effects of puddling intensity on the soil pore size distribution (a) and cumulative pore size distribution (b) quantified using X-ray CT imaging. The shaded areas are the standard error of the mean.

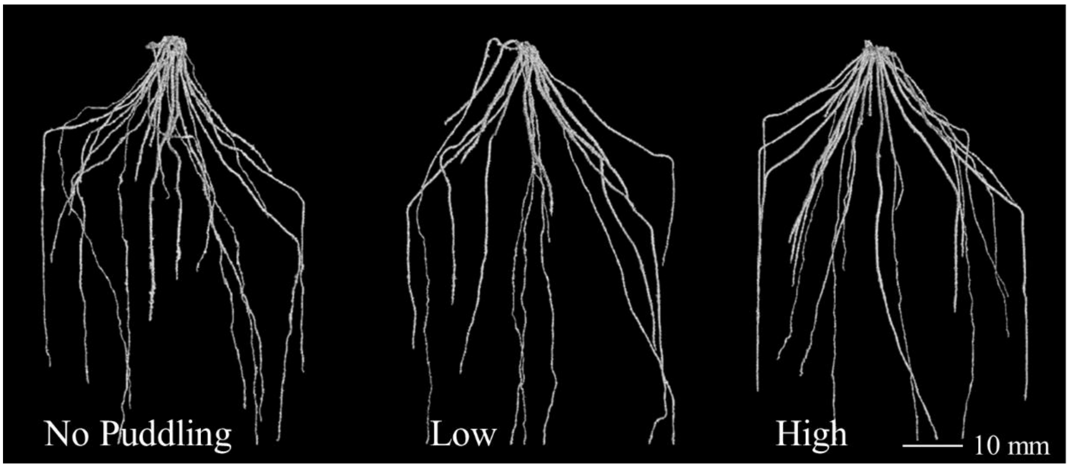

Figure 4. Representative three-dimensional root architecture acquired with X-ray CT imaging from different puddling intensities. Lateral roots were not observable due to the resolution.

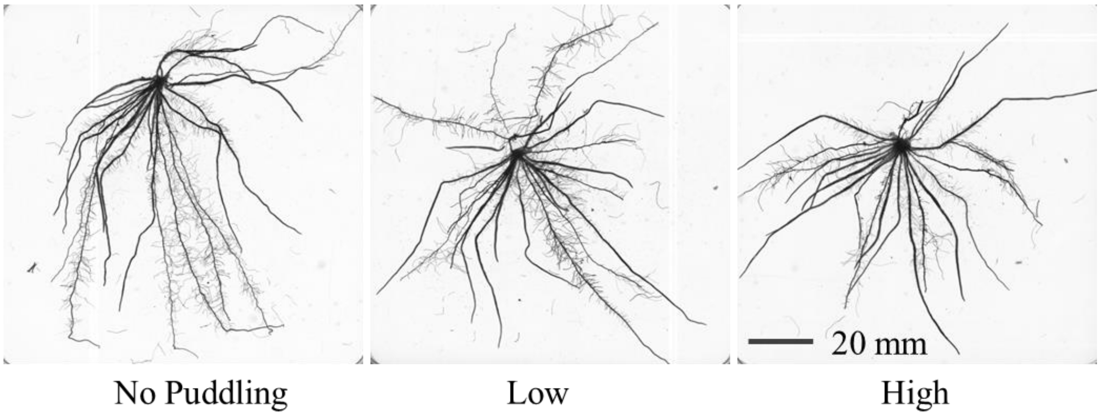

Figure 5. Representative two-dimensional root images from different puddling intensities.